



LAWRENCE
LIVERMORE
NATIONAL
LABORATORY

LLNL-TR-654027

Characterization of starting minerals to be used in kinetic experiments

S. Carroll, M. Smith, N. Marks, Z. Dai

May 8, 2014

Disclaimer

This document was prepared as an account of work sponsored by an agency of the United States government. Neither the United States government nor Lawrence Livermore National Security, LLC, nor any of their employees makes any warranty, expressed or implied, or assumes any legal liability or responsibility for the accuracy, completeness, or usefulness of any information, apparatus, product, or process disclosed, or represents that its use would not infringe privately owned rights. Reference herein to any specific commercial product, process, or service by trade name, trademark, manufacturer, or otherwise does not necessarily constitute or imply its endorsement, recommendation, or favoring by the United States government or Lawrence Livermore National Security, LLC. The views and opinions of authors expressed herein do not necessarily state or reflect those of the United States government or Lawrence Livermore National Security, LLC, and shall not be used for advertising or product endorsement purposes.

This work performed under the auspices of the U.S. Department of Energy by Lawrence Livermore National Laboratory under Contract DE-AC52-07NA27344.

Deliverable 1.1: Characterization of starting minerals to be used in kinetic experiments

LLNL FY14 AOP: The Viability of Sustainable, Self-Propping Shear Zones in Enhanced Geothermal Systems: Measurement of Reaction Rates at Elevated Temperatures

Susan Carroll, Megan Smith, Naomi Marks, Zurong Dai
Lawrence Livermore National Laboratory

Lawrence Livermore National Laboratory is expanding the geochemical for kinetic database for minerals identified in EGS shear stimulation zones to 300°C. In this report we present characterization data for select fracture filling minerals prior to reaction at elevated temperature. We have measured the surface area, chemical composition and crystal structure for illite, phlogopite, and biotite. We are currently purchasing smectite from a different source because our initial source proved to be of poor quality.

The minerals were ground and mechanically sieved and separated into the desired size fraction (150-250 μm). In keeping with previously published geochemical experimental work on similar layered silicates (e.g., Sass et al., 1987; Kohler et al., 2003), this size fraction was further treated with an acid wash to remove potential carbonate impurities (Zavarin et al., 2012). The mineral separates were then dried and re-sieved, and stored for further characterization analysis and kinetic experimentation.

Surface Area

Dissolution rates are normalized to mineral surface area. Initial surface areas of the unreacted 150 – 250 μm size fraction were measured with multi-point N_2 BET and are reported in Table 1. Based on feedback at program reviews from our modeling colleagues, we will also consider normalizing rates to geometric surface areas.

Table 1. Mineral source locations and the BET surface areas.

	Source	Location	BET Surface Area m^2/g
Illite: IMt-1	Source Clays Repository, Clay Minerals Society	Silver Hill, Montana, USA	34.2
Biotite/Phlogopite	Ward's Natural Science, NY	Not known	10.67
Muscovite	Ward's Natural Science, NY	Not known	4.23

Chemical Composition

The initial chemical composition was measured on individual grains mounted and polished for analysis on a JEOL JXA-8200 electron microprobe equipped with 5 wavelength-dispersive spectrometers, and a JEOL silicon-drift energy-dispersive spectrometer. Analyses were acquired using JEOL analysis software and x-ray correction was performed using the CITZAF correction. Operating conditions were 15 kV accelerating potential and 10 nA beam current, resulting in a beam/spot diameter of 5 μm . Orthoclase (Si,Al,K), Fe_2O_3 (Fe), spessartine (Mn), rutile (Ti), wollastonite (Ca), albite (Na), and MgO (Mg) silicate and oxide standards were used. Chemical composition was further confirmed by energy dispersive spectrometry during the transmission electron microscopy analysis using an energy-dispersive spectrometer.

Table 2. Measure illite, biotite/phlogopite, and muscovite compositions.

	Illite		Biotite/Phlogopite			Muscovite	
	LLNL TEM	LLNL EMP	LLNL TEM	LLNL EMP	Shao et al. 2011	LLNL TEM	LLNL EMP
K	1.65	1.55	2.03	1.88	2.00	1.76	1.74
Na		0.04		0.10			0.21
Ca		0.02					
Mg	0.68	0.54	5.58	5.28	5.74		
Mn							0.02
Fe	1.10	0.70	0.48	0.34		0.31	0.17
Al	4.16	4.15	2.40	2.49	2.46	6.50	5.88
Si	7.46	6.75	6.02	5.76	6.14	6.59	5.99
Ti		0.05	0.11	0.08			
O	24.00	24.00	23.10	24.00	22.00	24.00	24.00
H	4.00	4.00	3.10	4.00	2.00	4.00	4.00
F			0.90		2.00		

Table 2 compares the chemical composition determined with the electron microprobe (EMP) and the transmission electron microprobe (TEM) determined at LLNL. There is good agreement between the measurements. Although muscovite Al and Si numbers from the TEM analysis are systematically higher than those measured by EMP, the relative ratios of Al to Si yield values close to 1 and suggest that stoichiometric dissolution would yield equal concentrations of Al and Si on the molar scale. At the time of writing this report, we have decided to base stoichiometric dissolution on chemical formula determined by multiple EMP analyses, because results from the TEM analysis were typically taken from on spot only. Distribution of metals in the octahedral and tetrahedral site was based on an approach developed by Gaudette et al (1949).

Illite: $\text{K}_{1.55}(\text{Na}_{0.04}, \text{Ca}_{0.02})\text{Al}_{2.90}(\text{Fe}_{0.70}, \text{Mg}_{0.54}, \text{Ti}_{0.05})\text{Si}_{6.75}\text{Al}_{1.25}\text{O}_{20}(\text{OH})_4$

Biotite/Phlogopite: $\text{K}_{1.88}(\text{Na}_{0.10})(\text{Mg}_{5.28}\text{Fe}_{0.34}\text{Al}_{0.31}\text{Ti}_{0.08})(\text{Si}_{5.76}\text{Al}_{2.16})\text{O}_{20}(\text{OH})_4$

Muscovite: $\text{K}_{1.74}(\text{Na}_{0.21})\text{Al}_{3.88}(\text{Fe}_{0.17}\text{Mg}_{0.02})(\text{Si}_{5.99}\text{Al}_{2.00})\text{O}_{20}(\text{OH})_4$

Crystal Structure and Purity

Bulk mineralogy was confirmed from data collected from random orientation powder samples with a Bruker D8 Advance instrument using a Cu-K α source at 45 kV and 35 mA from 2° to 40° 2 θ in 0.01° steps. XRD cannot detect amorphous solids or minerals that are present at less than 2 wt%. Results are summarized in Figure 1. Crystal structure was further confirmed by TEM analysis in which specimens were prepared by the focus ion beam (FIB) technique. Mineral basal spacing was determined from high-resolution TEM image combining with fast Fourier transform analysis and electron diffraction. Results are summarized in Figure 2.

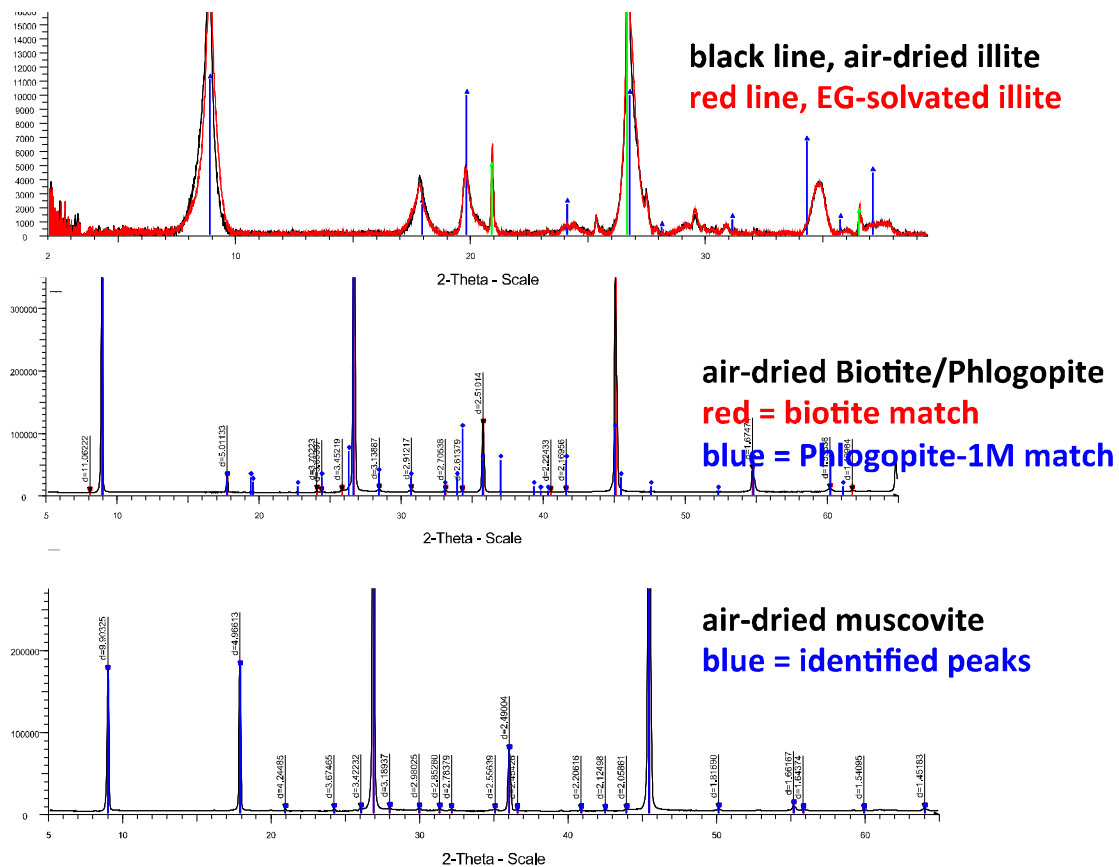


Figure 1. XRD patterns for illite (top), biotite/phlogopite (middle), muscovite (bottom).

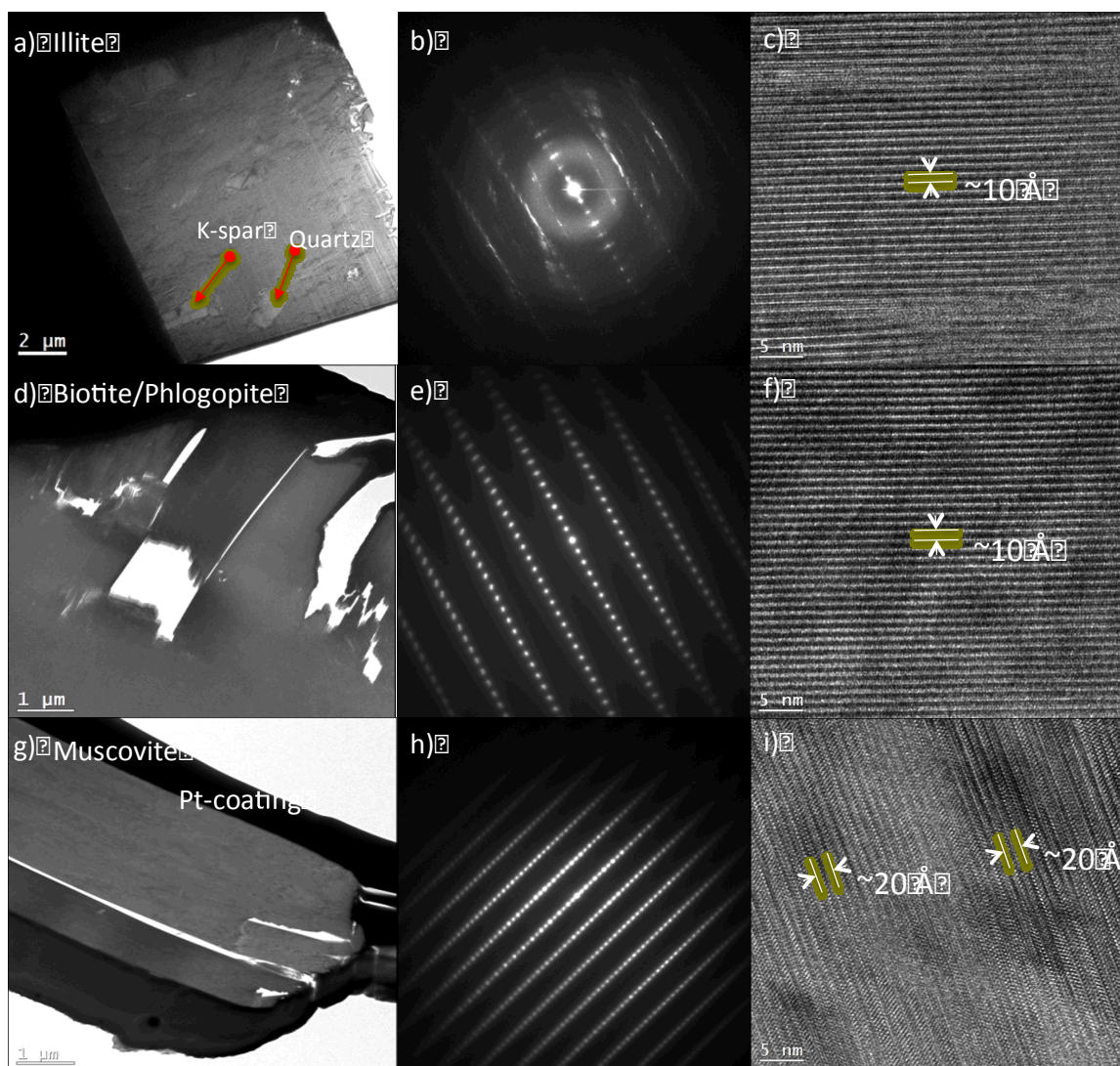


Figure 2. Summary of TEM analysis for illite (a, b, c), biotite (d, e, f), and muscovite (g, h, i) showing the thin sample (left column), the x-ray pattern (middle column) and the basal spacing (right column).

Illite contained some trace amounts of quartz and K-feldspar as detected in both powder diffraction pattern and in the TEM analysis. Comparison of XRD patterns for dry and ethylene glycolated samples show that the sample is predominately illite with no indication of expandable smectite clays. There is also no indication of other clays such as chlorite or vermiculite. TEM analysis confirmed illite crystal structure identified by XRD, as well as 10-Å basal spacing characteristic of this illite. We will consider the impact these impurities may have on the measured dissolution rates.

The biotite material selected for these kinetic experiments is the Mg-rich phlogopite end member. XRD and TEM analysis confirmed biotite/phlogopite crystal structure, as well as 10-Å basal spacing. No mineral impurities were

detected by TEM analysis for this sample.

Similar to the biotite/phlogopite, muscovite was well crystalline with no impurities detected by XRD or TEM. TEM analysis also confirmed 20-Å basal spacing.

References

1. Sass, BM, PE Rosenberg, and JA Kittrick, 1987. The stability of illite/smectite during diagenesis: An experimental study. *Geochim et Cosmochim Acta*, 51, 2103-15.
2. Kohler, SJ, F Dufaud, and EH Oelkers, 2003. An experimental study of illite dissolution kinetics as a function of pH from 1.4 to 12.4 and temperature from 5 to 50C, *Geochim et Cosmochim Acta*, 67, 3583-94.
3. Zavarin, M, BA Powell, M Bourbin, P Zhao, and AB Kersting, 2012. Np(V) and Pu(V) ion exchange and surface-mediated reduction mechanisms on montmorillonite, *Env Sci & Technol*, 46, 2692-8.